Available online at www.sciencedirect.com

ScienceDirect

Materials Today: Proceedings 17 (2019) 490–498

materialstoday: PROCEEDINGS

www.materialstoday.com/proceedings

6th International Conference on Functional Materials & Devices (ICFMD 2017)

Investigation of plasticized ionic conductor based on chitosan and ammonium bromide for EDLC application

M.F. Shukur[a,*], M.H. Hamsan[b], M.F.Z. Kadir[c]

[a]*Fundamental and Applied Sciences Department, Universiti Teknologi PETRONAS, 32610 Seri Iskandar, Perak, Malaysia*
[b]*Institute of Graduate Studies, University of Malaya, 50603 Kuala Lumpur, Malaysia*
[c]*Centre for Foundation Studies in Science, University of Malaya, 50603 Kuala Lumpur, Malaysia*

Abstract

Chitosan-based polymer electrolytes incorporated with ammonium bromide (NH_4Br) and glycerol were produced via solution casting technique. Characteristics of these electrolytes were examined using impedance technique, transport number measurement (TNM) and linear scan voltammetry (LSV). Based on the results obtained from impedance measurement, the sample with 40 wt.% glycerol achieved the highest ac and dc conductivies at room temperature. Dielectric behavior of the electrolytes was found to be improved upon incorporation of 40 wt.% glycerol, suggesting their relation with the conductivity trend. Result of TNM revealed that the conductivity has a huge contribution from ions. LSV analysis at 5 mV/s sweep rate showed that the best conducting sample is suitable for electrical double layer capacitor (EDLC) application. Specific capacitance (C_s) of the single carbon based electrode was determined from cyclic voltammetry (CV) technique.

Selection and peer-review under responsibility of Conference Committee Members of 6th International Conference on Functional Materials & Devices (ICFMD 2017).

Keywords: Polymer electrolyte; Chitosan; Ammonium bromide; Electrical double layer capacitor; Specific capacitance

* Corresponding author. Tel.: +605-3687156; fax: +605-3655905.
E-mail address: mfadhlullah.ashukur@utp.edu.my

Selection and peer-review under responsibility of Conference Committee Members of 6th International Conference on Functional Materials & Devices (ICFMD 2017).

1. Introduction

Ion conducting polymer is a class of solid type electrolyte that attract interest of researchers due to its potential electrochemical applications [1-4]. Synthetic polymers like polyvinylidene fluoride (PVdF) [5], polyethylene oxide (PEO) [6] and polyvinyl alcohol (PVA) [7] are often used as the host for ionic conduction. Nowadays, the use of biopolymers as the electrolyte host has attracted great attention of researchers. This is because these polymers are environmentally friendly and easily available at low cost [8]. Ion conducting biopolymers were reported to have good flexibility and transparency [9,10]. To act as a host for ionic conduction, a polymer should be able to dissolve salt. Chitosan is one of the well-known biopolymers for electrolyte host because it is a non-toxic and biodegradable material [11−13]. Chitosan contains oxygen and nitrogen atoms, whose lone pair electrons can provide the coordination sites for cations of salt [12]. In previous report [13], the incorporation of ammonium bromide (NH_4Br) into the chitosan based electrolytes shifted the IR band's peak of carboxamide and amine band region, proving the coordination of cation at oxygen and nitrogen atoms of chitosan.

Polymer electrolytes usually obtain lower ionic conductivity than that of liquid electrolyte. This is due to crystallinity of polymer as well as poor motion performance of the polymer backbones [14]. A lot of techniques e.g. plasticization, incorporation of nanofiller and polymer blending have been used to seek the improvement in conductivity and other characteristics of polymer electrolyte. Plasticizers with high dielectric constant can improve the salt dissociation and the mobility of ions [15]. The improvement in salt dissociation will increase the number of ionic species which in turn enhance the conductivity. Besides, incorporation of plasticizer can provide an alternative pathway for conduction such that the motion of ions can be decoupled from the local motion of the host [12]. In the present work, glycerol was chosen as plasticizer since it has functional hydroxyl groups which can assist the salt dissociation [16]. Our earlier report focused on the conductivity analysis of the chitosan based polymer electrolytes [13]. In this paper, further characterizations are reported and the electrolyte with optimum conductivity is employed in the construction of an electrical double layer capacitor (EDLC). To the best of our knowledge, the application of plasticized chitosan−NH_4Br electrolyte in EDLC has never been reported.

2. Methodology

2.1. Samples preparation

The procedures to prepare the plasticized electrolytes have been described in [13]. Table 1 shows the designation and composition of the polymer electrolytes.

Table 1. Composition and designation of electrolytes.

Designation	Composition of chitosan-NH_4Br-glycerol				
	Weight of chitosan-NH_4Br (g)				
	Chitosan	NH_4Br	Weight percentage of chitosan-NH_4Br (wt.%)	Weight of glycerol (g)	Weight percentage of glycerol (wt.%)
G0	1.000	0.429	100	0	0
G10	1.000	0.429	90	0.159	10
G20	1.000	0.429	80	0.357	20
G30	1.000	0.429	70	0.612	30
G40	1.000	0.429	60	0.952	40
G50	1.000	0.429	50	1.429	50

2.2. Electrical impedance spectroscopy (EIS)

EIS is a well-known technique for measuring impedance of a material. In the present work, HIOKI 3532-50 LCR HiTESTER (50 Hz $\leq f \leq$ 1 MHz) was employed to conduct the impedance measurements. Prior to the measurements, two stainless steel discs were used to sandwich the samples. The measurements were performed at room temperature. The data collected from this experiment was used to examine the conductivity and dielectric behaviors of the samples.

2.3. Transport number measurement

The transport numbers of electron (t_e) and ion (t_{ion}) were measured using dc polarization method [17]. Two stainless steel electrodes were used to sandwich the sample. A digital dc power supply (V&A Instrument DP3003) was used to polarize the cell at a constant voltage of 0.20 V across the polymer electrolyte [18,19]. The change in current as a function of time was monitored.

2.4. Linear scan voltammetry (LSV)

The purpose of LSV technique is to evaluate the stable working potential range for the best conducting sample. Thus, this technique was conducted by using Digi-IVY DY2300 potentiostat at 5 mV/s sweep rate. Stainless steel working and reference/counter electrodes were used. The LSV technique was performed at room temperature.

2.5. Carbon based electrodes preparation

A mixture of 6 wt.% carbon black (Super P), 13 wt.% polyvinylidene fluoride (PVdF) and 81 wt.% activated carbon (RP20) was stirred in N-methylpyrrolidone (NMP) (EMPLURA) to prepare the electrode slurry. The slurry was then coated on an aluminium foil. The coated electrode was heated at 60 °C for drying process.

2.6. Fabrication and characterization of EDLC

The EDLC was constructed by employing the best conducting sample to separate the identical carbon based electrodes. The EDLC cell was clamped between two Perspex plates for characterization purpose. Cyclic voltammetry (CV) measurements of the EDLC were conducted using a potentiostat (Digi-IVY DY2300) in the voltage range of 0 to 0.85 V at different sweep rates [20-23]. The measurements were performed at room temperature.

3. Results and discussion

3.1. Ac and dc conductivities

From the impedance spectroscopy, the frequency dependence conductivity or ac conductivity (σ_{ac}) of the sample was determined using the following equation:

$$\sigma_{ac} = \frac{d}{A}\left(\frac{Z_r}{Z_r^{\,2} + Z_i^{\,2}}\right) \tag{1}$$

Here, A is the area of electrolyte−electrode interface, d is the sample thickness, Z_r is the real impedance and Z_i is the imaginary impedance. The plot of σ_{ac} against frequency is represented in Fig. 1. Each plot consists of two distinct regions. At the region of f < 100 kHz, the conductivity increases with the increase in frequency. It is known that electrodes polarization or accumulation of ions at the interfaces occurs at low frequencies, providing a low number

of free mobile ions. The amount of ions accumulated at the interfaces is decreased as the frequency increases. Thus, at f < 100 kHz, the number of mobile ions available for transportation increases with increasing frequency which leads to

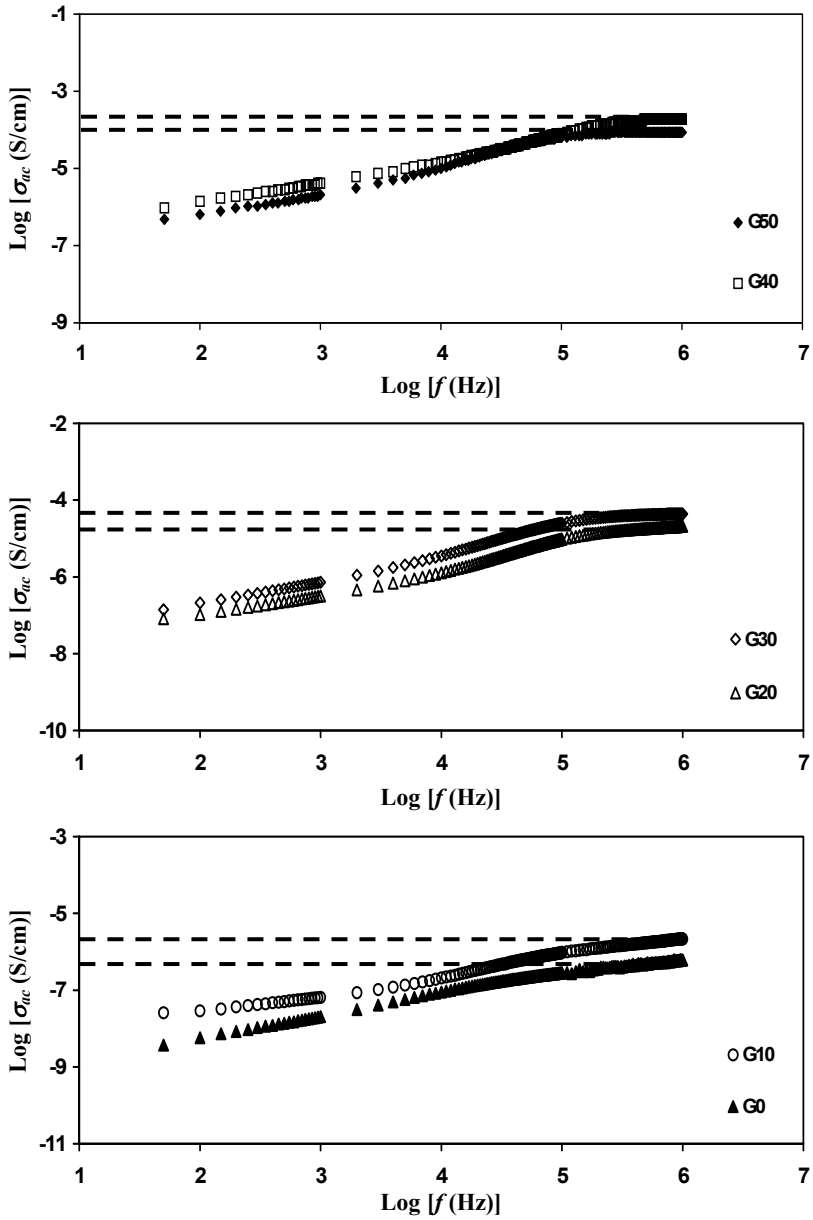

Fig. 1. Variation of ac conductivity with frequency at room temperature.

an increase in σ_{ac} [24]. However, σ_{ac} is observed to be nearly frequency independent at f > 100 kHz. The frequency independent conductivity is correlated with the dc conductivity (σ_{dc}) [25]. By extrapolating the plateau region to zero frequency, the σ_{dc} of the samples can be determined. The values of σ_{dc} obtained from σ_{ac} plots are tabulated in Table 2. The results agree well with the values obtained using bulk resistance [13]. At all frequencies, it can be observed that σ_{ac} and σ_{dc} of G40 is the highest. Addition of plasticizer has created alternative pathways for ion conduction leading to conductivity enhancement [26]. Besides, the addition of glycerol promotes ion dissociation which decreases the formation of ion aggregates and increases the number of mobile charge carriers. This

phenomenon enhances the σ_{ac} and σ_{dc}. On addition of 50 wt.% glycerol, the decrease in σ_{ac} and σ_{dc} may be caused by the formation of linkages between the molecules of plasticizer causing the salt to recrystallize, resulting in a conductivity decrement [27]. This result verifies the ionic conductivity result in [13].

Table 2. Dc conductivity from ac conductivity plot.

Sample	σ_{dc} (S/cm)
G0	4.2×10^{-7}
G10	1.7×10^{-6}
G20	2.1×10^{-5}
G30	4.3×10^{-5}
G40	1.9×10^{-4}
G50	8.5×10^{-5}

3.2. Dielectric analysis

Analysis on the dielectric behavior of ion conducting polymers helps us to understand the polarization effect at the electrolyte–electrode interface [28]. The dielectric behavior of the samples has been determined by calculating the following parameters:

$$\varepsilon_r = \frac{Z_i}{\omega C_o (Z_r^{\ 2} + Z_i^{\ 2})} \tag{2}$$

$$\varepsilon_i = \frac{Z_r}{\omega C_o (Z_r^{\ 2} + Z_i^{\ 2})} \tag{3}$$

Here, ε_r is the dielectric constant, ε_i is the dielectric loss, C_o is the capacitance in vacuum and ω is the angular frequency. ε_r is resulted from the total polarization arising from the trapped charges as well as dipoles in the electrolytes [29]. ε_i is resulted from dissipation of energy due to the polarization effect and motion of charge carriers [24]. From Fig. 2a, the ε_r value of G40 is the highest, showing that the sample has more charges than the other samples. In our previous report [13], the conductivity is optimized at 40 wt.% glycerol concentration. A report by Aziz et al. [30] showed that dielectric constant result of phthaloyl chitosan–ammonium thiocyanate (NH_4SCN) electrolyte is in agreement with the conductivity trend. When plasticizer is incorporated into the sample, the degree of ion combination is reduced while the degree of ion dissociation is increased that results in conductivity enhancement as shown in our previous work [13]. According to Ramesh et al. [31], plasticized sample with a greater conductivity has a greater ε_r value. In Fig. 2b, it is observed that the trend of ε_i is similar to ε_r. The decrease in ε_r and ε_i with frequency increment is ascribed to the tendency of dipoles in the polymer chains to orient themselves in the applied electric field direction [32]. At the high frequency region, the rapid reversal of the applied electric field causes the decrease in electrode polarization thus decreases the ε_r and ε_i [31].

3.3. Transport number analysis

The t_e and t_{ion} are essential parameters in understanding the conductivity of materials. Since polymer electrolytes are ionic conductor, t_{ion} of the electrolyte should be greater than the t_e, indicating the dominancy of ions to the total conductivity. To determine t_e, stainless steel discs were used as the electrodes since electrons are transparent to the ion blocking stainless steel electrodes [33]. For an ionic conductor, the current flows through the electrode will fall rapidly with time, while for a non-ionic conductor, the current would not decrease with time [1]. The plot of

polarization current as a function of time for G40 is presented in Fig. 3. It is observed that the current decreases rapidly before attained a steady state at 0.1 μA. This phenomenon indicates that the sample is an ionic conductor. By knowing t_e, the value of t_{ion} was determined using:

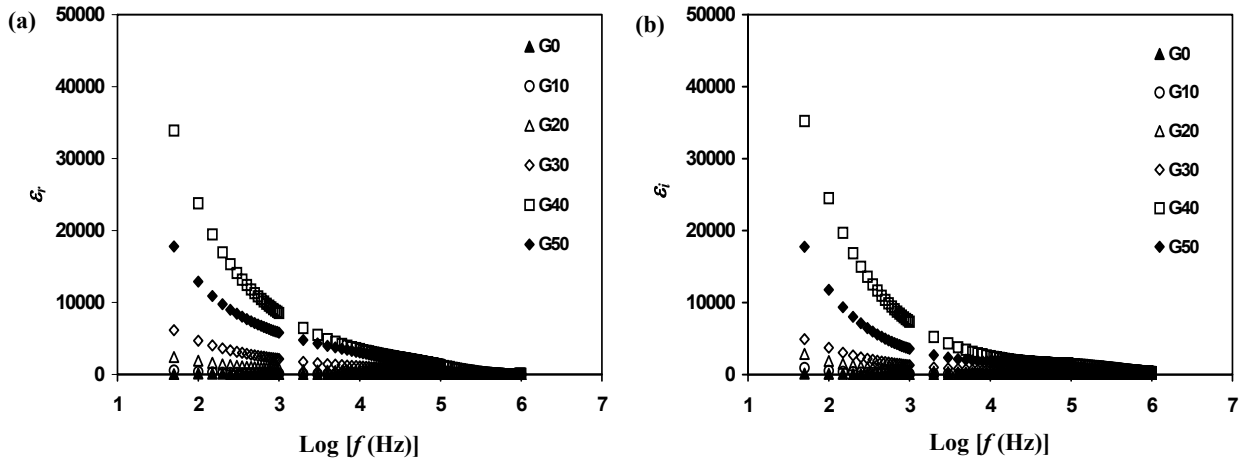

Fig. 2. Plots of (a) ε_r and (b) ε_i against frequency.

$$t_{ion} = 1 - t_e \tag{4}$$

or

$$t_{ion} = \frac{I_o - I_{ss}}{I_o} \tag{5}$$

The t_e and t_{ion} for the sample are found to be 0.02 and 0.98, respectively. These results confirm ions as the major conducting species.

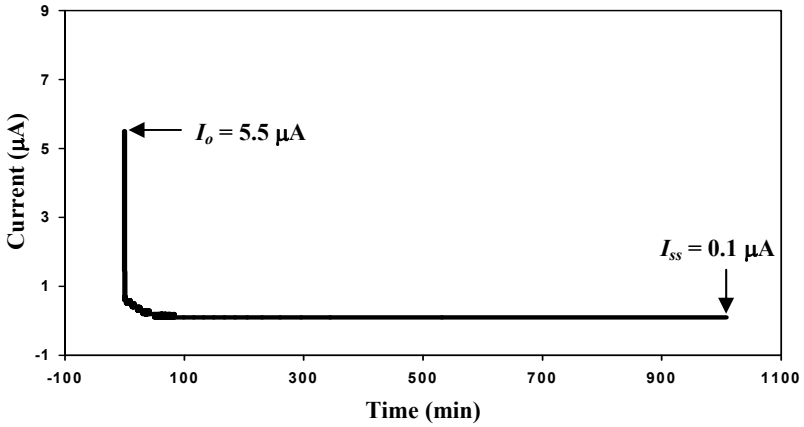

Fig. 3. Transference number of G40 using stainless steel electrodes.

3.4. LSV analysis

LSV technique aimed to evaluate the maximum working potential of G40. Polymer electrolyte for EDLC must be stable within the range of its operating potential and show no degradation peak over the potential range. Fig. 4 shows the linear sweep voltammogram of G40. It can be observed that the decomposition potential of A40 is 1.80 V, which is sufficient for a common EDLC. Plasticized starch−chitosan−ammonium chloride (NH_4Cl) electrolyte is reported to decompose at 1.65 V and was used for EDLC application in the voltage range of 0 to 0.85 V [1]. According to Shuhaimi et al. [23], the decomposition potential of methyl cellulose−ammonium nitrate (NH_4NO_3) is ~ 1.5 V. The authors have used the electrolyte for application in an EDLC in the voltage range of 0 to 0.85 V. LSV result in this work indicates that the A40 is suitable for EDLC application.

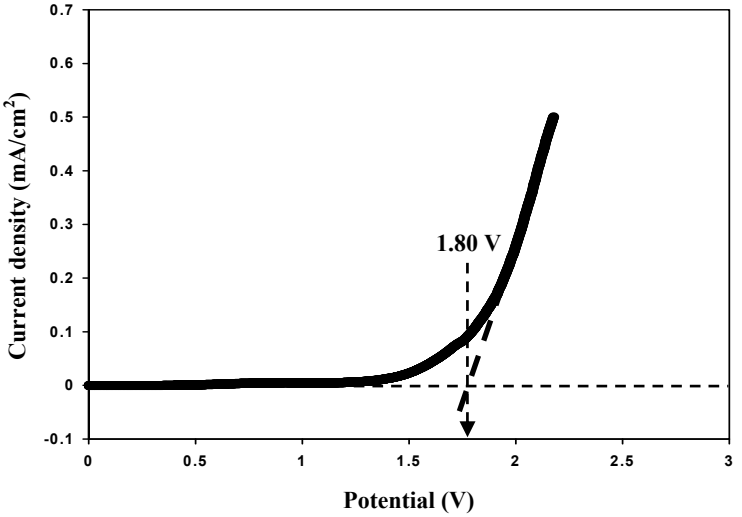

Fig. 4. Linear sweep voltammogram for G40 at 5 mV/s sweep rate.

3.5. EDLC characterization

EDLC performance was analyzed by CV at various sweep rates. In Fig. 5, when the sweep rate is decreased from 100 mV/s to 10 mV/s, the cyclic voltammogram turns from leaf like shape to almost rectangular shape. It is observed that the shape of the voltammogram deviates from an ideal rectangle as the sweep rate increases. This result can be attributed to the carbon porosity and internal resistance, thus producing a current dependence of the potential [34]. At slower sweep rate, almost rectangular shape without redox peaks can be seen indicating that the charge storage is due to the accumulation of ions at the electrolyte−electrode interfaces. This type of charge storage is known as double layer capacitance [35]. The values of specific capacitance (C_s) of the single carbon based electrode at different sweep rates were determined from the following equation:

$$C_S = \frac{2}{(V_f - V_i)mv}\int_{V_i}^{V_f} I(V)dV \tag{6}$$

where (V_f-V_i) is the potential window, $\int I(V)\,dV$ is the integral area of the cyclic voltammogram, v is the applied sweep rate while m is the mass of active material in a single electrode. The result is tabulated in Table 3. The C_s is found to increase with the decrease in sweep rate. As the sweep rate decreases, there is an increase in the number of charge stored on the electrode surface which in turn decreases the energy loss [36]. At slower sweep rates, the higher value of C_s can be attributed to the fact that ionic carriers can utilize the vacant sites in the electrode active material since

Table 3. Specific capacitance at various sweep rates.

Sweep rate (mV/s)	C_s (F/g)
100	4.4
50	5.3
20	6.5
10	7.5

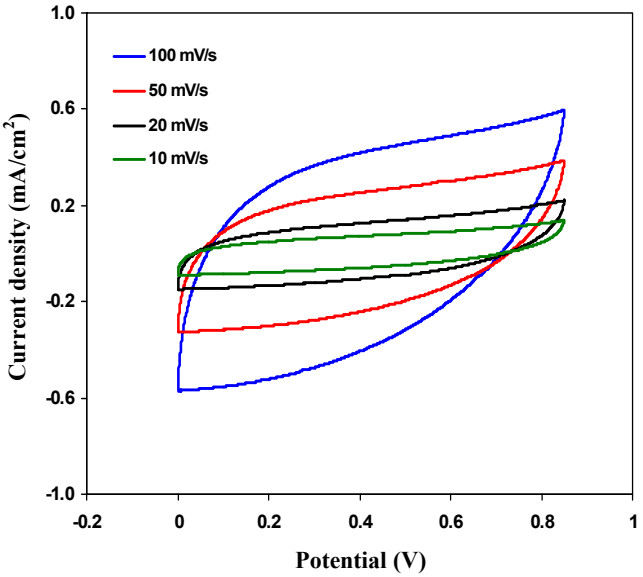

Fig. 5. Cyclic voltammogram of the EDLC at different sweep rates.

they have enough time to diffuse into the vacant sites [37]. The sweep rate dependent behavior showed by the present EDLC is a characteristic of capacitor cells [38].

4. Conclusions

Plasticized NH_4Br doped chitosan electrolyte samples were successfully prepared via solution casting technique. The highest conducting electrolyte with 40 wt.% glycerol content (G40) exhibited the highest ac and dc conductivies at room temperature. The addition of glycerol improved the dielectric properties of the polymer electrolytes as G40 electrolyte obtained the highest dielectric constant. Ionic transport number measurement revealed that G40 electrolyte is an ionic conductor with ionic transport number of 0.98 at room temperature. LSV analysis revealed that G40 electrolyte decomposed at 1.80 V, indicating that the highest conducting electrolyte is suitable for EDLC application. The present EDLC has been analyzed using CV technique. At 10 mV/s, C_s of a single electrode is found to be 7.5 F/g. The results in the present work showed the potential of plasticized chitosan−NH_4Br as an electrolyte in the EDLC application.

Acknowledgements

The authors thank the Universiti Teknologi PETRONAS for the Short Term Internal Research Fund (STIRF) support (Grant no.: 0153AA-F90), the University of Malaya for the Bantuan Kecil Penyelidikan (BKP) support (Grant no.: BKS005-2018) and the Malaysian Ministry of Higher Education for the Fundamental Research Grant Scheme (FRGS) support (Grant no.: FP009-2015A) provided.

References

[1] M.F. Shukur, M.F.Z. Kadir, Electrochim. Acta 158 (2015) 152−165.
[2] M.H. Khanmirzaei, S. Ramesh, K. Ramesh, Ionics 21 (2015) 2383-2391.
[3] J. Mindemark, B. Sun, E. Torma, D. Brandell, J. Power Sources 298 (2015) 166-170.
[4] N. Shaari, S.K. Kamarudin, J. Power Sources 289 (2015) 71-80.
[5] P. Tamilselvi, M. Hema, Physica B 437 (2014) 53-57.
[6] M.L. Verma, H.D. Sahu, I, Ionics 21 (2015) 3223-3231.
[7] J. Malathi, M. Kumaravadivel, G.M. Brahmanandhan, M. Hema, R. Baskaran, S. Selvasekarapandian, J. Non-Cryst. Solids 356 (2010) 2277-2281.
[8] N. Kulshrestha, P.N. Gupta, Ionics 22 (2016) 671–681.
[9] R. Alves, J.P. Donoso, C.J. Magon, I.D.A. Silva, A. Pawlicka, M.M. Silva, J. Non-Cryst. Solids 432 (2016) 307-312.
[10] A.S. Samsudin, H.M. Lai, M.I.N. Isa, Electrochim. Acta 129 (2014) 1-13.
[11] R. Leones, F. Sentanin, S.C. Nunes, J.M.S.S. Esperanca, M.C. Goncalves, A. Pawlicka, V.D.Z. Bermudez, M.M. Silva, Electrochim. Acta 184 (2015) 171-178.
[12] S. Navaratnam, K. Ramesh, S. Ramesh, A. Sanusi, W.J. Basirun, A.K. Arof, Electrochim. Acta 175 (2015) 68-73.
[13] M.F. Shukur, M.S. Azmi, S.M.M. Zawawi, N.A. Majid, H.A. Illias, M.F.Z. Kadir, Phys. Scripta T157 (2013) 014049-014054.
[14] F.I. Chowdhury, M.U. Khandaker, Y.M. Amin, M.Z. Kufian, H.J. Woo, Ionics 23 (2017) 275–284.
[15] S. Rajendran, M. Sivakumar, R. Subadevi, Mater. Lett. 58 (2004) 641-649.
[16] T. Bourtoom, Songklanakarin J. Sci. Technol. 30 (2008) 149-165.
[17] J.B. Wagner, C.J. Wagner, J. Chem. Phys. 26 (1957) 1597-1601.
[18] H.J. Woo, S.R. Majid, A. K. Arof, Mater. Res. Innov. 15 (2011) S49-S54.
[19] M. H. Hamsan, M. F. Shukur, M.F.Z. Kadir , Ionics 23 (2017) 1137-1154.
[20] S.N. Asmara, M.Z. Kufian, S.R. Majid, A.K. Arof, Electrochim. Acta. 57 (2011) 91-97.
[21] N.E.A. Shuhaimi, L.P. Teo, H.J. Woo, S.R. Majid, A.K. Arof, Polym. Bull. 69 (2012) 807-826.
[22] M.H. Hamsan, M.F. Shukur, M.F.Z. Kadir, Ionics 23 (2017) 3429-3453
[23] N.E.A. Shuhaimi, S.R. Majid, A.K. Arof, Mater. Res. Innov. 13 (2009) 239-242.
[24] S. Ramesh, C.−W. Liew, Measurement 46 (2013) 1650-1656.
[25] Z. Osman, M.I.M. Ghazali, L. Othman, K.B.M. Isa, Results Phys. 2 (2012) 1–4.
[26] A. Pawlicka, A.C. Sabadini, E. Raphael,D.C. Dragunski, Mol. Cryst. Liq. Cryst. 485 (2008) 804–816.
[27] M.R. Johan, L.M. Ting, Int. J. Electrochem. Sci. 6 (2011) 4737–4748.
[28] H.J. Woo, S.R. Majid, A.K. Arof, Mater. Chem. and Phys. 134 (2012) 755-761.
[29] S.R. Majid, R.C. Sabadini, J. Kanicki, A. Pawlicka, Mol. Cryst. Liq. Cryst. 604 (2014) 84-95.
[30] N.A. Aziz, S.R. Majid, A.K. Arof, J. Non-Cryst. Solids 358 (2012) 1581-1590.
[31] S. Ramesh, A.H. Yahaya, A.K. Arof, Solid State Ionics 152-153 (2002) 291-294.
[32] H. Nithya, S. Selvasekarapandian, D.A. Kumar, A. Sakunthala, M. Hema, P. Christopherselvin, J. Kawamura, R. Baskaran, C. Sanjeeviraja, Mater. Chem. Phys. 126 (2011) 404-408.
[33] M.Z. Kufian, M.F. Aziz, M.F. Shukur, A.S. Rahim, N.E. Ariffin, N.E.A. Shuhaimi, S.R. Majid, R. Yahya, A.K. Arof, Solid State Ionics 208 (2012) 36−42.
[34] M.F.Z. Kadir, A.K. Arof, Mater. Res. Innov. 15 (2011) S217-S220.
[35] G. Ma, E. Feng, K. Sun, H. Peng, J. Li, Z. Lei, Electrochim. Acta 135 (2014) 461-466.
[36] M. Nasibi, M.A. Golozar, J. Power Sources, 206 (2012) 108-110.
[37] C.-S. Lim, K.H. Teoh, C.-W. Liew, S. Ramesh, Ionics, 20 (2014) 251-258.
[38] S.A. Hashmi, A. Kumar, S.K. Tripathi, J. Phys. D Appl. Phys. 40 (2007) 6527-6534.